

ChemComm

Accepted Manuscript



This is an *Accepted Manuscript*, which has been through the Royal Society of Chemistry peer review process and has been accepted for publication.

Accepted Manuscripts are published online shortly after acceptance, before technical editing, formatting and proof reading. Using this free service, authors can make their results available to the community, in citable form, before we publish the edited article. We will replace this *Accepted Manuscript* with the edited and formatted *Advance Article* as soon as it is available.

You can find more information about *Accepted Manuscripts* in the [Information for Authors](#).

Please note that technical editing may introduce minor changes to the text and/or graphics, which may alter content. The journal's standard [Terms & Conditions](#) and the [Ethical guidelines](#) still apply. In no event shall the Royal Society of Chemistry be held responsible for any errors or omissions in this *Accepted Manuscript* or any consequences arising from the use of any information it contains.

COMMUNICATION

A Heterodinuclear RuIr Metal Complex for direct Imaging of rRNA in living cells

Cite this: DOI: 10.1039/x0xx00000x

 Shiguo Sun,^{*a} Jitao Wang,^a Daozhou Mu,^a Jingyun Wang,^b Yongming Bao,^b Bo Qiao^a and Xiaojun Peng^{*a}

Received 00th January 2014,

Accepted 00th January 2014

DOI: 10.1039/x0xx00000x

www.rsc.org/

A novel dual luminescence (523 nm, 615 nm) heterodinuclear complex RuIr for RNA detection was developed, which was successfully used to image RNA in living cells.

To detect cellular RNA and RNA-regulated processes, it is necessary to employ techniques that provide information regarding the expression and localization of RNA in living cells.¹⁻⁴ Of the various analytical techniques, fluorescence staining using RNA-binding molecules offers enormous advantages in terms of simplicity, sensitivity, and specificity.⁵⁻⁹ However, in contrast to numerous fluorescent DNA probes, RNA probes for cell imaging are rarely reported.¹⁰ At present, SYTO RNA-Select, a green fluorescent cellular stain, is the only commercially available nucleolar stain¹¹ that shows significantly enhanced luminescence upon RNA binding.¹² However, the drawbacks of this dye include single color emission and photobleaching, which severely handicap its application; moreover, the structure of this commercial dye has not yet been published.¹³ Hence, there is a high demand for novel live cell RNA imaging probes.

Of the many different types of dyes and metal complexes, particularly iridium and ruthenium complexes, have attracted a lot of attention because of their desirable properties, such as high Stokes shifts, pronounced photostability, color-tunable luminescence, and long emission lifetimes.¹⁴⁻¹⁸ For example, the iridium complexes have been used as probes for live cell imaging, by virtue of their rapid uptake by living cells and localization property.¹⁹⁻²¹ Li and coworkers reported an iridium complex that rapidly (incubation time < 10 min) concentrated in the nuclei of living cells²⁰, and Lo *et al.* also found that iridium dipyridoquinoxaline complexes could be taken up by MDCK cells and stain the nucleolus²¹. On the other hand, ruthenium complexes have been extensively studied as luminescent probes over the past few decades because of their rich photophysical properties.²²⁻²⁴ For example, Barton *et al.* reported a ruthenium complex conjugated to a cell-penetrating peptide to facilitate entry into the nucleus.²⁵ Thomas *et al.* reported a dinuclear ruthenium(II) polypyridyl complex that functioned as a structure-sensitive probe for the direct imaging of DNA in cells.²⁶ All these observations suggest that ruthenium complexes have the potential to be used as a cellular marker and probe.

In our previous work, a flexible, saturated carbon chain was employed to covalently link the two ruthenium moieties together, resulting in a synergistic increase in properties of the two intramolecularly linked ruthenium activating centers.^{27, 28} Continuing our research efforts in the same direction in the current study, a heterodinuclear metal complex [Ru(bpy)₃-(CH₂)₁₀-Ir(F₂ppy)₂]³⁺ (ppy = 1-phenyl-pyridine; bpy = 2, 2'-bipyridine), designated hereafter as **RuIr** (Fig. 1), was designed and synthesized; it contains an iridium(I) moiety covalently linked to a ruthenium(II) moiety through a 10-carbon chain. The iridium(I) moiety was chosen because it could both function as the donor for energy transfer and be used to promote the cellular uptake of probes, whereas the ruthenium(II) moiety is the acceptor of energy transfer, such that the two moieties together provide a ratiometric response. For comparison purposes, the corresponding dimetallic complexes [Ru(bpy)₃-(CH₂)₁₀-Ru(bpy)₃]⁴⁺ and [Ir(F₂ppy)₂-(CH₂)₁₀-Ir(F₂ppy)₂]²⁺ (ppy = 1-phenyl-pyridine; bpy = 2, 2'-bipyridine), designated as **RuRu** and **IrIr**, respectively (Fig. S1), were synthesized as control. Our results demonstrate that **RuIr** exhibits dual luminescence (523 nm and 615 nm), and can be successfully taken up by live MCF-7, HeLa, and LO2 cells. **RuIr** can interact with RNA, which triggers a significant luminescence enhancement from iridium(I) moiety, resulting in a rapid enhancement of emission intensity from the nucleoli of living cells, whereas the ruthenium(II) moiety serves as an acceptor for the energy transfer, resulting in a ratiometric luminescence response.

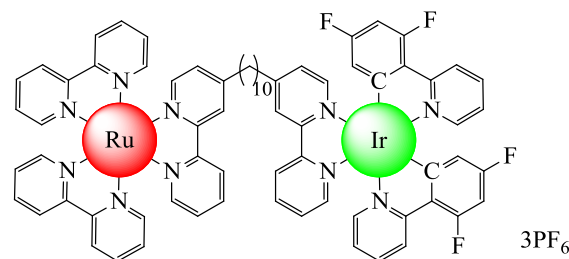


Fig. 1 The chemical structure of **RuIr**.

The absorption and emission spectra of **RuIr**, **RuRu**, and **IrIr** at room temperature are shown in Fig. 2. A solution of **RuRu** in acetonitrile shows two typical absorption bands, one in the visible

region with a maximum wavelength at 457 nm because of **RuRu** metal-to-ligand charge transfer (MLCT) and the other at 275–300 nm, assignable to $\pi-\pi^*$ transition.^{29–31} In contrast, a solution of **IrIr** shows absorption bands at 250–350 nm, which is attributable to $F_2\text{ppy}$ -centered $\pi-\pi^*$ transition.^{19, 32, 33} **RuIr**, on the other hand, exhibits absorption properties of both the activating centers, and its absorption intensity is nearly half that of **RuRu** and **IrIr**. Upon excitation at 458 nm, the dinuclear ruthenium complex **RuRu** exhibits a strong emission band at 615 nm, whereas the dinuclear iridium complex **IrIr** shows a strong emission at 523 nm upon excitation at 350 nm (Fig. 2). **RuIr**, on the other hand, exhibits dual emissions at both 523 nm and 615 nm with excitation at 405 nm, owing to the presence of both the iridium and ruthenium activating centers. The emission intensity at 615 nm is nearly half that of the bimetallic ruthenium complex **RuRu**, while the emission intensity at 523 nm is much weaker than that of **IrIr**, mostly because the photons emitted by the iridium fluorophore could be absorbed by the ruthenium fluorophore.^{34, 35}

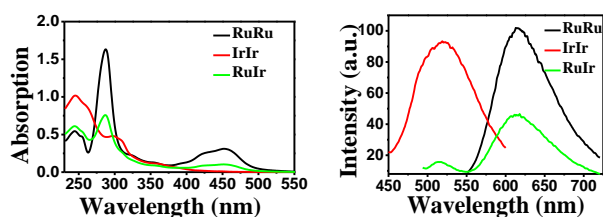


Fig. 2 UV-Vis absorption (left) and fluorescence emission (right) spectra of the complexes **RuIr**, **IrIr** and **RuRu** in CH_3CN , at a concentration of 2×10^{-6} M.

A luminescence decay experiment performed at room temperature determined the fluorescence lifetime of **RuIr** to be 375.2 ns (Fig. S2). This long fluorescence lifetime offer advantages over SYTO RNA-Select (fluorescence lifetime = 1.9 ns) (Fig. S3). Fig. S4 shows that **RuIr** displayed excellent photostability in solution after 25 min irradiation under a 500 W iodine-tungsten lamp. This is in contrast to SYTO RNA-Select, which demonstrates significant fading after 5 minutes exposure time. These outstanding properties make **RuIr** suitable for microscopy imaging of living cells in long-duration studies.

We next assessed the response of these three complexes to RNA, and found it to be dissimilar. In the presence of 80-fold excess RNA, **RuRu** shows only a slight increase in luminescence intensity (Fig. 3a and S5), suggesting a low binding affinity toward RNA, while the luminescence of **IrIr** is quenched by RNA (Fig. 3b and S6). The **RuIr** complex, on the other hand, exhibits significant spectral changes when RNA is introduced into the sample (Fig. 3c). In the absence of RNA, the emission intensity of the iridium center is much lower than that of the ruthenium center. With the addition of RNA, however, the emission from the ruthenium center is quenched, while that from the iridium center is increased. The $I_{\text{Ir}}/I_{\text{Ru}}$ ratio is increased over 6.3 fold upon addition of 80-fold excess RNA, providing a good ratiometric response (Fig. S7). A linear calibration curve between the $I_{\text{Ir}}/I_{\text{Ru}}$ ratio and RNA amount was established over the RNA concentration range 1.2×10^{-5} – 1.4×10^{-4} mol/L (Fig. S8). The regression equation was $(I_{\text{min}} - I)/(I_{\text{min}} - I_{\text{max}}) = 4.39963 + 0.91437 \times \log[\text{RNA}]$, with a linear coefficient $R = 0.99144$, where “I” refers to $I_{\text{Ir}}/I_{\text{Ru}}$; the RNA detection limit attained was 1.5×10^{-5} mol/L. In control experiments using DNA, not much difference was observed in emission spectra in the presence or absence of DNA, suggesting a low binding affinity of **RuIr** toward DNA (Fig. S9). When treated with excess RNA, DNA, chymotrypsin, lysozyme, BSA, HSA, and protease, **RuIr** displays a

much higher affinity for RNA compared to the other biomacromolecules, as shown in Fig. S10, which suggests that the complex **RuIr** can be employed as a probe for RNA.

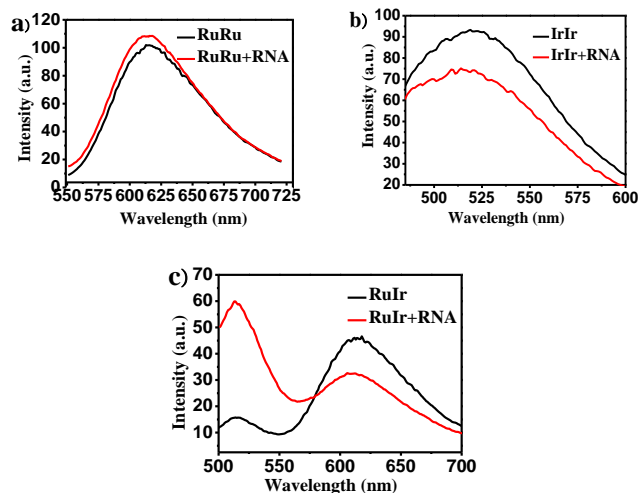


Fig. 3 Emission spectra of a) **RuRu**, b) **IrIr**, and c) **RuIr**, at 2.0 μM concentration in phosphate-buffered saline (PBS; pH 7.5, 20 mM) at 298 K, in the presence or absence of 80-fold excess RNA.

The yeast RNA used in experiment is total RNA, which consists of rRNA, mRNA and small RNAs (like tRNA and miRNA). Among them, mRNA is comprising only about 1–5% of the total RNA³⁶, and it is very sensitive to degradation after extraction^{37,38}. Considering that the main composition of yeast RNA is ribosomal RNA, in control experiment, tRNA, one kind of small RNAs from baker’s yeast, was measured to test the selectivity of **RuIr** according to the literature³⁹. As shown in Fig. S11, not much emission response of **RuIr** to a 80-fold excess tRNA can be observed, indicated that rRNA, accounting for about 80% of total RNA, induced the fluorescence changes of **RuIr**. The exclusive commercial available RNA selective probe named SYTO RNA-Select was also taken as a control here. As shown in Fig. S12, treatment of SYTO RNA-Select with yeast RNA and tRNA induced similar enhancement on luminescence intensity at 560 nm, indicated that SYTO RNA-Select is actually lack of selectivity to various RNA.

Considering that Uracil is a RNA-specific nitrogen base⁴⁰, the interactions of **RuIr** with four different base sequences, poly(dA-dT), poly(dG-dC), poly(dA-dU), and poly(dU), were further examined by luminescence measurement, to determine the key factors involved in the interaction process of **RuIr** upon RNA binding. As shown in Fig. S13, the addition of these base sequences induced little changes in **RuIr** luminescence, suggesting that the luminescence change is not associated with the uracil-containing RNA backbone. Therefore, these observations suggest that the change in emission intensities of **RuIr** might be attributed to the possible secondary and tertiary structures of RNA. It is known that the stabilization of the secondary and tertiary structures of RNA will be affected by temperature of the surrounding environment^{41,42}, we then performed the luminescence detection of **RuIr** with RNA under different temperature. As shown in Fig. 4, along with the increasing of the temperature, the emission of ruthenium moiety was decreased while that of iridium moiety was increased. When the temperature was reached 95 $^{\circ}\text{C}$, the emission of the iridium moiety at 523 nm was decreased as time going on, because the RNA would gradually lose their native 2D and 3D structures.

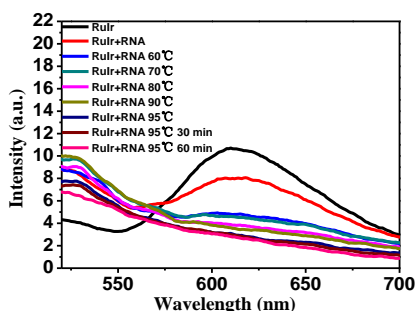


Fig. 4 The luminescent spectra of **RuIr** (0.33 μM) with the presence of 60 eq RNA in phosphate buffered saline (PBS) (pH=7.5, 20 mM) under different temperature.

To further figure out the interaction between **RuIr** and the secondary and tertiary structures of RNA, the role of ionic concentration on the luminescence titrations were done in phosphate buffered saline (PBS) (pH=7.5, 20 mM), the results are shown in Fig. S14 and S15. In the case of **RuIr** alone, the emission of iridium moiety was increased while that of ruthenium moiety was decreased along with the increasing concentration of KI (0-140 equiv) and NaCl (0-100 equiv). With the presence of 60 equiv RNA, the same trend can be followed on that of iridium moiety; however, not much difference can be observed on the emission of ruthenium moiety. These results provide some further evidence that the luminescence change was due to the specific interactions of **RuIr** with the secondary and tertiary structures of RNA.

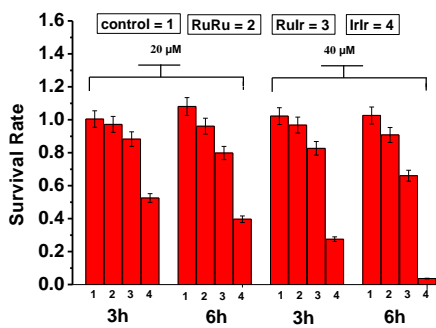


Fig. 5 The cell toxicity of **RuRu**, **RuIr**, **IrIr**.

As shown in Fig. 5, after incubation with **RuIr** for 3 h and 6 h at concentration of 20 μM , the cellular survival rate was estimated to be about 88% and 80%, respectively, suggesting low cytotoxicity of **RuIr** at the imaging concentration. Therefore, for validation of the use of **RuIr** in vivo cell imaging, three cell types, including two cancer cell lines (MCF-7 and HeLa) and one normal cell line (LO2), were employed for bioimaging. Excitation wavelengths of 405 nm and 458 nm were used, and the emissions measured at 510-560 nm and 590-640 nm, so that the green and red emissions could be examined separately. In live MCF-7 cells, the dye was distributed throughout the cell (20 μM , 2 h), and the luminescence was localized within certain cellular regions, notably the nucleoli and cytoplasm of the cells (Fig. 6a). The luminescence intensity in the nucleoli was found to be about 2.2 times higher than that of the cytoplasm (Fig. 6c). Similar trends were also observed in the normal cell line LO2 and the cancer cell line HeLa (Fig. S16).

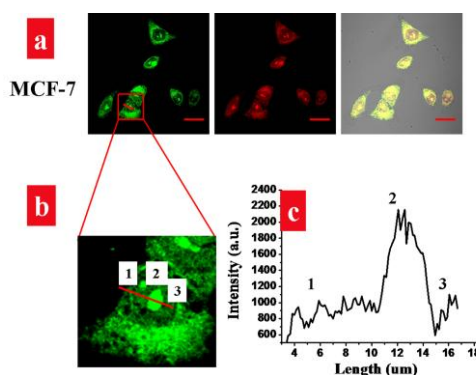


Fig. 6 a) Cellular uptake of **RuIr** (20 μM) when incubated with live MCF-7 cells for 2 h at 37 $^{\circ}\text{C}$. From left to right: green channel (510–560 nm), red channel (590–640 nm), and overlay images. b) Magnified view of confocal luminescence images of live MCF-7 cells incubated with 20 μM **RuIr** for 2 h. c) Luminescence intensity profile along the line shown in panel b. Scale bar : 20 μm .

In contrast to **RuIr**, no staining of live MCF-7 cells was observed with **RuRu** under the same conditions (20 μM , 2 h), probably due to the hydrophilicity and positive charge (+4) of **RuRu** (Fig. S17a). Figure S17b shows that although **IrIr** (20 μM , 2 h) can easily diffuse across the cell membrane, no staining of the nucleoli was observed during subsequent imaging; this is in agreement with its aforementioned binding performance with RNA in vitro.

Treatment with deoxyribonuclease (DNase) and ribonuclease (RNase), which would selectively hydrolyze only DNA and RNA, respectively, in the cell, was conducted to further confirm the staining of RNA by **RuIr** (Fig. S18). MCF-7 cells were fixed in methanol for these experiments. In the DNase-treated cells, nucleolar staining by the complex **RuIr** remains mostly unaltered, whereas the luminescence intensity in nucleoplasm is dramatically diminished. On the other hand, RNase treatment dramatically diminishes **RuIr** luminescence (Fig. S18c), further demonstrating that the emissions observed in the microscopy studies with **RuIr** result from the interactions of the complex with RNA.

The nucleolar localization of **RuIr** was further confirmed by colocalization experiments. Upon treatment of fixed and permeabilized MCF-7 cells with **RuIr** and the commercially available nucleolar stain SYTO RNA-Select, bright yellow spots, denoting colocalization, were observed in the nucleoli in the overlay image (Fig. S19a). Figure S19b shows the result of experiments examining the colocalization of **RuIr** and the DNA stain Hoechst 33258. The red luminescence corresponding to the nucleoli and cytoplasm further demonstrates the RNA-staining ability of **RuIr**.

Conclusions

In conclusion, a luminescent heterodinuclear complex, **RuIr**, exhibiting dual-emissive properties (523 nm and 615 nm) was developed, and a linear calibration curve between the $I_{\text{Ir}}/I_{\text{Ru}}$ ratio and RNA amount was established. Cell imaging validates the use of **RuIr** as a cellular marker and an RNA probe.

Notes and references

^a State Key Laboratory of Fine Chemicals, Dalian University of Technology, E 224 West Campus, No. 2, Linggonglu, 116024, Dalian, China. Fax & Tel: +86-411-84986304; E-mail: shiguo@dlut.edu.cn, pengxj@dlut.edu.cn

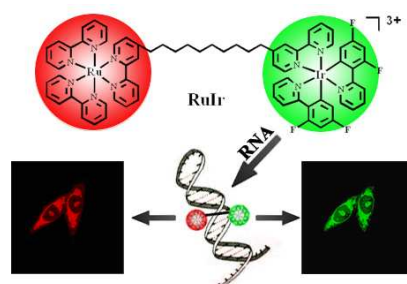
^b School of Life Science and Biotechnology, Dalian University of Technology, No. 2, Linggonglu, 116024, Dalian, China.

This work was financially supported by State Key Laboratory of Fine Chemicals, Dalian University of Technology, the Education Ministry and National Natural Science Foundation of China (Nos. 21306019, 21072024, 20872012), National Key Technology R&D Program (2011BAE07B06) and National Basic Research Program of China (2009CB724706).

† Electronic Supplementary Information (ESI) available: [details of any supplementary information available should be included here]. See DOI: 10.1039/b000000x/

‡ Footnotes should appear here. These might include comments relevant to but not central to the matter under discussion, limited experimental and spectral data, and crystallographic data.

- 1 B. A. Armitage, *Curr. Opin. Chem. Biol.* 2011, **15**, 806-812.
- 2 R. W. Dirks, C. Molenaar and H. J. Tanke, *Methods* 2003, **29**, 51-57.
- 3 S. Kummer, A. Knoll, E. Socher, L. Bethge, A. Herrmann and O. Seitz, *Bioconjugate Chem.* 2012, **23**, 2051-2060.
- 4 X. Li, Z. Li, A. A. Mart, S. Jockusch, N. Stevens, D. L. Akins, N. J. Turro and J. Ju, *Photochem. Photobiol. Sci.* 2006, **5**, 896.
- 5 M. Baker, *nat. methods*, 2012, **9**, 787-790.
- 6 S. Berndl, M. Breunig, A. Göpferich, H.-A. Wagenknecht, *Org. Biomol. Chem.* 2010, **8**, 997.
- 7 R. W. Dirks and H. J. Tanke, *Chem. Biol.* 2006, **13**, 559-561.
- 8 M. S. T. Gonçalves, *Chem. Rev.* 2009, **109**, 190.
- 9 A. Kobori, T. Ueda, Y. Sanada, A. Yamayoshi, A. Murakami, *Biosci., Biotechnol., Biochem.* 2013, **77**, 1117.
- 10 A. Erve, Y. Saoudi, S. Thiroit, C. Guetta-Landras, J.-C. Florent, C.-H. Nguyen, D. S. Grierson and A. V. Popov, *Nucleic Acids Res.*, 2006, **34**.
- 11 Q. Li, Y. Kim, J. Namm, A. Kulkarni, G. R. Rosania, Y.-H. Ahn and Y.-T. Chang, *Chem. Biol.* 2006, **13**, 615-623.
- 12 J. Yu, D. Parker, R. Pal, R. A. Poole, M. J. Cann, *J. Am. Chem. Soc.* 2006, **128**, 2294.
- 13 R. P. Haulgland, 2005, 710.
- 14 H.-j. Yu, Y. Chen, L. Yu, Z.-f. Hao and L.-h. Zhou, *Eur. J. Med. Chem.* 2012, **55**, 146-154.
- 15 B. Yu, Y. Chen, C. Ouyang, H. Huang, L. Ji and H. Chao, *Chem. Commun.* 2013, **49**, 810.
- 16 B. Tong, M. Zhang, Z. Han, Q. Mei and Q. Zhang, *J. Organomet. Chem.* 2013, **724**, 180-185.
- 17 F. L. Thorp-Greenwood, R. G. Balasingham and M. P. Coogan, *J. Organomet. Chem.* 2012, **714**, 12-21.
- 18 F. L. Thorp-Greenwood, *Organometallics*, 2012, **31**, 5686-5692.
- 19 W. Jiang, Y. Gao, Y. Sun, F. Ding, Y. Xu, Z. Bian, F. Li, J. Bian, C. Huang, *Inorg. Chem.* 2010, **49**, 3252.
- 20 C. Li, M. Yu, Y. Sun, Y. Wu, C. Huang, F. Li, *J. Am. Chem. Soc.* 2011, **133**, 11231.
- 21 K. Y. Zhang, S. P.-Y. Li, N. Zhu, I. W.-S. Or, M. S.-H. Cheung, Y.-W. Lam and K. K.-W. Lo, *Inorg. Chem.* 2010, **49**, 2530-2540.
- 22 M. R. Gill, J. A. Thomas, *Chem. Soc. Rev.* 2012, **41**, 3179.
- 23 R. Zhang, Z. Ye, Y. Yin, G. Wang, D. Jin, J. Yuan, J. A. Piper, *Bioconjugate Chem.* 2012, **23**, 725.
- 24 B. Jing, M. Zhang, T. Shen, *Spectrochim. Acta, Part A* 2004, **60**, 2635.
- 25 C.A. Puckett, J.K. Barton, *Journal of the American Chemical Society*, 2009, **131**, 8738-8739.
- 26 M. R. Gill, J. Garcia-Lara, C. Smythe, G. Battaglia and J. A. Thomas, *Nat. Chem.* 2009, **1**, 662-667.
- 27 S. Sun, Y. Yang, F. Liu, Y. Pang, J. Fan, L. Sun and X. Peng, *Anal. Chem.* 2009, **81**, 10227-10231.
- 28 S. Sun, F. Li, F. Liu, X. Yang, J. Fan, F. Song, L. Sun and X. Peng, *Dalton Trans.* 2012, **41**, 12434.
- 29 W. Zhang, R. Zhang, J. Zhang, Z. Ye, D. Jin and J. Yuan, *Anal. Chim. Acta* 2012, **740**, 80-87.
- 30 C. Núñez, C. Silva López, O. N. Faza, J. Fernández-Lodeiro, M. Diniz, R. Bastida, J. L. Capelo, C. Lodeiro, *JBIC, J. Biol. Inorg. Chem.* 2013, **18**, 679.
- 31 M. Matson, F. R. Svensson, B. Nordén, P. Lincoln, *J. Phys. Chem. B* 2011, **115**, 1706.
- 32 K. Y. Zhang and K. K.-W. Lo, *Inorg. Chem.* 2009, **48**, 6011-6025.
- 33 L. Xiong, Q. Zhao, H. Chen, Y. Wu, Z. Dong, Z. Zhou and F. Li, *Inorg. Chem.* 2010, **49**, 6402-6408.
- 34 N. A. O'Connor, N. Stevens, D. Samaroo, M. R. Solomon, A. A. Marti, J. Dyer, H. Vishwasrao, D. L. Akins, E. R. Kandel, N. J. Turro, *Chem. Commun.* 2009, 2640-2642.
- 35 N. Stevens, N. O'Connor, H. Vishwasrao, D. Samaroo, K. E. R., D. L. Akins, C. M. Drain, N. J. Turro, *J. Am. Chem. Soc.* 2008, **130**, 7182-7183.
- 36 J. Sambrook, D. W. Russell, 2001. *Molecular Cloning: A Laboratory Manual*, 3rd edn. Cold Spring Harbor Laboratory Press, Cold Spring Harbor.
- 37 S. A. Bustin, *J. Mol. Endocrinol.* 2002, **29**, 23-39.
- 38 S. Fleige, V. Walf, S. Huch, C. Prgomet, J. Sehm, *Biotechnol Lett.* 2006, **28**, 1601-1613.
- 39 Y. Liu, E. J. Jun, G. Kim, A. Lee, J. Lee and J. Yoon, *Chem. Commun.* 2014, **50**, 2505-2507.
- 40 J.C. Lee and R.R. Gutell, *J. Mol. Biol.* 2004, **344**, 1225-1249.
- 41 I. Jr. Tinoco and C. Bustamante, *J. Mol. Biol.* 1999, **293**, 271-281.
- 42 N. Tian, Y. Yang and Y. Jin, *Nucleic Acids Res.*, 2011, 5669-5861.



A novel dual luminescence **RuIr** for RNA detection was developed, which was successfully used to image RNA in living cells.